Two-Dimensional Nanoparticle Arrays Derived from Ferritin Monolayers

ARTICLE *in* LANGMUIR · MAY 2007

Impact Factor: 4.46 · DOI: 10.1021/la062891f · Source: PubMed

5 AUTHORS, INCLUDING:

Dimiter Petsev
University of New Mexico
96 PUBLICATIONS **2,764** CITATIONS
SEE PROFILE

Brian Prevo
Nike Inc.
18 PUBLICATIONS **1,246** CITATIONS
SEE PROFILE

Plamen Atanassov
University of New Mexico
337 PUBLICATIONS **5,297** CITATIONS
SEE PROFILE

Two-Dimensional Nanoparticle Arrays Derived from Ferritin Monolayers

Zhen Yuan,† Dimiter N. Petsev,† Brian G. Prevo,‡ Orlin D. Velev,‡ and Plamen Atanassov*,†

Department of Chemical and Nuclear Engineering, University of New Mexico, Albuquerque, New Mexico 87131, and Department of Chemical Engineering, North Carolina State University, Raleigh, North Carolina 27695

Received October 2, 2006. In Final Form: February 28, 2007

A scalable technique for making silica coatings with embedded two-dimensional arrays of iron oxide nanoparticles is presented. The iron oxide nanoparticle arrays were formed by depositing quasi-crystalline ferritin layers, an iron storage protein with an iron oxide mineral core, on solid substrates by a spread-coating technique based on evaporation-induced convective assembly. The layer of protein molecular arrays was then encapsulated in a silica matrix film deposited from a sol precursor. The organic protein shell of the ferritin molecules was then removed by controlled pyrolysis, leaving ordered iron oxide cores bound in the silica matrix. This article is the first report on combining convective self-assembly of proteins with sol−gel techniques of oxide film formation. The technique is technologically feasible and scalable to make coatings of encapsulated ordered magnetic clusters tens of cm^2 or larger in size.

Introduction

Two-dimensional protein arrays are of substantial interest due to their potential applications in structure analysis,[1,2] surface architectures for sensing, and nanoelectronics and nanostructured templates for magnetic devices or microengineered catalytic materials.[3] Encapsulating protein into inorganic host materials as hybrid bioinorganic matrixes provides a versatile approach to incorporating and preserving their functionality for different applications, typically as selective coatings for optical and electrochemical biosensors, solid-phase biocatalysts, and others.[4−7]

One of the earlier approaches to the preparation of ordered two-dimensional protein arrays was implemented at air/liquid interfaces.[3,8−13] In these studies, the ordered protein arrays were transferred to a carbon film (with varying degrees of fidelity) and dried on the solid substrate. This multistep deposition method is complex, inefficient, and difficult to scale up. The proteins can be easily removed from the surface by slight mechanical perturbation. It is of significant importance to reduce the process to a single operation that would directly form two-dimensional proteins arrays on solid surfaces and would encapsulate the arrays in a thin inorganic matrix in order to facilitate potential applications.

In this article we describe how ordered two-dimensional arrays of ferritin, an iron-storage protein with iron oxide core, can be deposited in a direct, rapid, and controlled process on solid substrates and further immobilized in a silica matrix to yield nanocoatings with arrays of magnetic domains. The protein molecules are self-assembled into a two-dimensional hexagonally ordered structure from an aqueous solution by the liquid convection due to evaporation. Such thin bioinorganic composite films could find applications as microengineered catalysts and electrocatalysts, robust biosensor architectures, and molecular electronic[14−16] and nanoelectronic devices.[17]

Adachi and Nagayama reported that protein arrays can be directly formed on solid substrate by deposition from a wetting film of protein solution on the surface.[18] However, this report failed to demonstrate long-range order and the deposition technique described was highly dependent on the tool precision. In this study, we used a deposition process based on similar principles to form self-assembled, ordered 2D arrays of protein on solid surfaces. We designed a coating system allowing rapid deposition of large-scale protein crystal films from minimal volume of suspension. The technique was previously reported to controllably deposit 2D colloidal crystals from polystyrene microspheres.[19] Colloidal crystals are spatially ordered materials with sub-micrometer periodicity that have potential for applications in processing and storing optical information, magnetic memories, advanced coatings, catalysis, and other emerging nanotechnologies.[20−22] By addition of a durable matrix material,

* Corresponding author. E-mail: plamen@unm.edu. Fax: 505-277-5433.

† University of New Mexico.

‡ North Carolina State University.

(1) Jap, B. K.; Zulauf, M.; Scheybani, T.; Hefti, A.; Baumeister, W.; Aebi, U.; Engel, A. *Ultramicroscopy* **1992**, *46*, 45.

(2) Yoshimura, H.; Matsumoto, M.; Endo, S.; Nagayama, K. *Ultramicroscopy* **1990**, *32*, 265.

(3) Nagayama, K. *Adv. Biophys.* **1997**, *34*, 3.

(4) Avnir, D.; Braun, S.; Lev, O.; Ottolenghi, M. *Chem. Mater.* **1994**, *6*, 1605.

(5) Jin, W.; Brennan, J. D. *Anal. Chim. Acta* **2002**, *461*, 1.

(6) Dave, B. C.; Miller, J. M.; Dunn, B.; Vallentine, J. S.; Zink, J. I. *J. Sol-Gel Sci. Technol.* **1997**, *8*, 629.

(7) Gill, I. *Chem. Mater.* **2001**, *13*, 3404.

(8) Fromherz, P. *Nature* **1971**, *231*, 267.

(9) Denkov, N. D.; Velev, O. D.; Kralchevsky, P. A.; Ivanov, I. B.; Yoshimura, H.; Nagayama, K. *Nature* **1993**, *361* (6407), 26.

(10) Yamashita, I. *Thin Solid Films* **2001**, *393*, 12.

(11) Scheybani, T.; Yoshimura, H.; Baumeister, W.; Nagayama, K. *Langmuir* **1996**, *12* (2), 431.

(12) Yoshimura, H.; Scheybano, T.; Baumeister, W.; Nagayama, K. *Langmuir* **1994**, *10*, 3290.

(13) Nagayama, K.; Takeda, S.; Endo, S.; Yoshimura, H. *Jpn. J. Appl.* **1995**, *34*, 3947.

(14) Falkner, J. C.; Turner, M. E.; Bosworth, J. K.; Lin, T. W.; Johnson, J.; Colvin, V. L. *Abstr. Pap. Am. Chem. Soc.* **2003**, *225* (2), U51.

(15) Colvin, V. L.; Turner, M. E.; Bosworth, J. K.; Falkner, J. C. *Abstr. Pap. Am. Chem. Soc.* **2003**, *225* (2), U154.

(16) Velev, O. D.; Kaler, E. W.; Lenhoff, A. M. *Adv. Mater.* **1999**, *11* (16), 1345.

(17) Miura, A.; Hikono, T.; Matsumura, T.; Yano, H.; Hatayama, T.; Uraoka, Y.; Fuyuki, T.; Yoshii, S.; Yamashita, I. *Jpn. J. Appl. Phys.* **2006**, *45* (1), L1.

(18) Adachi, E.; Nagayama, K. *Langmuir* **1996**, *12*, 1836.

(19) Prevo, B. G.; Velev, O. D. *Langmuir* **2004**, *20* (6), 2099.

(20) Velev, O. D.; Kaler, E. W. *Adv. Mater.* **2000**, *12* (7), 531.

(21) Kulinowski, K. M.; Jiang, P.; Vaswani, H.; Colvin, V. L. *Adv. Mater.* **2000**, *12* (11), 833.

10.1021/la062891f CCC: $37.00
Published on Web 04/03/2007

which infiltrates and solidifies in the lattice voids, the colloidal crystal structures can be replicated without destroying the order of the crystal.[20−23] Removing the original colloidal particles leaves a new type of material that contains pores arranged in long-range periodic structure produced by the original colloidal crystal.[24,25] Thus, colloidal crystal templating is a viable approach for creating ordered nanostructured materials. Here we have extended this approach down to the nanometer domain by encapsulation of the ferritin arrays in a silica matrix and removing the organic protein component to obtain a two-dimensional assembly of iron oxide cores.

The extension of the colloidal templating to protein arrays on substrates in our study is facilitated by the fact that large globular proteins have sizes that cross the boundary between molecular and colloidal scales and demonstrate properties that are similar to colloidal systems.[26] The arrays were assembled from ferritin, a large globular iron-storage protein found in most living organisms, provided that sufficient iron is present.[27] It is a 4:3:2 symmetrical spherical aggregate of 24 polypeptide chains. The monomer ferritin has a molecular diameter of 10−13 nm, with a hollow 6−8 nm diameter interior where up to 4500 iron atoms can be stored, forming a mineral core.[27−29] When fully formed, this iron core consists primarily of iron oxide (ferrihydrite) with a specific amount of phosphates.[29] We have chosen ferritin for our initial experiments because of its well-defined known structure, globular (nearly spherical) shape, and unique capacity to carry and sterically protect an inorganic (mineral) core, a sort of biologically synthesized nanocluster. Combining this coating and encapsulation approach with biological methods of altering the composition of the inorganic core nanocluster of the native ferritin molecules[30,31] presents an opportunity to design new bio-derived materials for a variety of applications.

There are literature examples pointing out that sol−gel-derived silica structure is a feasible material for hybrid bioinorganic matrixes.[4−7,32,33] Sol−gel encapsulation is a process of physical entrapment, and sol−gel-derived materials can be synthesized at room temperature as well as under mild reaction conditions. Sol−gel entrapment of proteins provides means for creating bio-inorganic composite materials that take advantage of this well-developed chemistry. It allows integration of biological functionality with mesoporous silica structure to yield complex bio-inorganic architectures.[34,35] Encapsulation in silica was an essential step in the process of turning the ferritin coatings into usable solid-state material reported in this study. After the ferritin molecules were immobilized on the surface, controlled pyrolysis could be used to remove the organic protein shell. This can be followed by chemical reduction (in a hydrogen furnace, for example) to obtain metal nanoparticles from the oxide cores.

Experimental Section

Materials. All chemicals were obtained from Aldrich and used without further purification unless noted elsewhere.

Ferritin Purification and Solution Preparation. To prepare the sample for deposition, the commercial ferritin product was purified through a Biologic Duo-Flow Chromatography system. One milliliter of holoferritin (Sigma Co., Ltd.) solution was gel-filtered (Sephacryl S-400 HR, Amersham Pharmacia Biotech) in buffer solution of pH 8.0 containing 50 mM Tris HCl and 150 mM NaCl, using a Millipore chromatography column VL11 x 500. Only the elution peak for ferritin monomers was collected to exclude dimers or trimers, which could obstruct the two-dimensional crystallization. The purified ferritin solution was stored at 4 °C to prevent subsequent aggregation. The actual deposition was performed at room temperature, but the time needed for the experiment was much shorter than the one needed for dimerization and aggregation to occur. The monomer solution was concentrated by centrifugation (5000 rpm, 2−3 °C) three times for 25 minc each after adjusting the pH to 8.0 and changing buffer to deionized (DI) water. Before the deposition process, the purified ferritin solutions (about 100 mg/mL) were diluted to 0.5−20 mg/mL.

Si-Wafer/Glass Slide Pretreatment. Both Si wafers and microscope slides were kept in piranha solution (30% H_2O_2:96−98% H_2SO_4 = 1:3) at least overnight and rinsed with DI water to make the surface hydrophilic and then dried by blowing N_2 gas.

Protein-Deposition and Incorporation Process. The top left frame of Figure 1 illustrates the scheme for direct assembly of structured films of ferritin molecules on solid substrates by evaporation-induced convective assembly. An aliquot amount of 10−15 μL of ferritin solution (0.5−20 mg/mL) as-prepared is placed at the junction of two microscopy slides or silicon wafers held at an angle of 23 ± 1° to form a meniscus along the line of contact. The electric linear motor (as illustrated at the bottom of Figure 1) pushes the moving plate (droplet plate) and drags the solution across the substrate at a constant velocity (in the range from 1.6 to 76 μm/s depending on the concentration of the ferritin solution chosen) at ambient temperature and controlled humidity. The device is placed in a controlled-humidity box, equipped with an aerosol-type humidifier and a hygrometer; and the relative humidity is maintained at 30−40%. The film is formed and dried on the substrate as the solvent evaporates.

Silica (stock) sol was prepared by mixing tetraethyl orthosilicate (TEOS), ethanol (200 proof), DI water, and HCl (0.07 N) followed by a reaction at 60 °C for 90 min.[36] For each dip coating, 0.25 mL of stock sol was diluted with 0.043 mL of water and 0.6 mL of ethanol and stirred well to yield a sol with final proportion of TEOS/ethanol/water/HCl = 1:20:5.02:0.0007, and the pH was adjusted to 7. The silica layer was then deposited via traditional dip coating (Figure 1, top right) using a low withdrawal velocity of 1−3 cm/s directly over the as-deposited ferritin array film without any additional treatment at room temperature.

Controlled Pyrolysis. The silicon wafer/microscope slide with ferritin array (with and without silicate coating) was heated in the center of a quartz tube in an electronic oven at 450 °C for 2 h. Pure nitrogen gas (99.999% N_2) was flowed through the system to avoid further oxidation of Fe(II) to Fe(III).

Characterization. The morphology of the deposited ferritin arrays (before and after pyrolysis) was studied by scanning electron microscopy (SEM) using Hitachi S-4800 and S-5200 operating at acceleration voltage of 2.0−15 kV and transmission electron microscopy (TEM) using a JEOL 2010 high-resolution transmission electron microscope (HRTEM) and a JEOL 2010F FASTEM field emission gun scanning transmission electron microscope (STEM). Energy-dispersive spectroscopy (EDS) mapping (obtained as a part

(22) Colvin, V. L. *MRS Bull.* **2001**, *26* (8), 637.
(23) Velev, O. D.; Lenhoff, A. M. *Curr. Opin. Colloid Interface Sci.* **2000**, *5*, 56.
(24) Jiang, P.; Cizeron, J.; Bertone, J. F.; Colvin, V. L. *J. Am. Chem. Soc.* **1999**, *121*, 7957.
(25) Tessier, P. M.; Velev, O. D.; Kalambur, A. T.; Lenhoff, A. M.; Rabolt, J. F.; Kaler, E. W. *Adv. Mater.* **2001**, *13* (6), 396.
(26) Yau, S. T.; Petsev, D. N.; Thomas, B. R.; Vekilov, P. G. *J. Mol. Biol.* **2000**, *303* (5), 667.
(27) Massover, W. H. *Micron* **1993**, *24* (4), 389.
(28) Harrison, P. M.; Arosio, P. *Biochim. Biophys. Acta* **1996**, *1275*, 161. Lawson, D. M.; Treffry, A.; Artymiuk, P. J.; Harrison, P. M.; Yewdall, S. J.; Luzzago, A.; Cesareni, G.; Levi, S.; Arosio, P. *FEB* **1989**, *254* (1,2), 207.
(29) Harrison, P. M.; Andrews, S. C.; Artymiuk, P. J.; Ford, G. C.; Guest, J. R.; Hirzmann, J.; Lawson, D. M.; Livingstone, J. C.; Smith, J. M. A.; Treffry, A.; Yewdall, S. J. *Adv. Inorg. Chem.* **1991**, *36*, 449.
(30) Wong, K. K. W.; Mann, S. *Adv. Mater.* **1996**, *8* (11), 928.
(31) Douglas, T.; Stark, V. T. *Inorg. Chem.* **2000**, *39* (8), 1828.
(32) Ellerby, L. M.; Nishida, C. R.; Nishida, F.; Yamanaka, S. A.; Dunn, B.; Valentine, J. S.; Zink, J. I. *Science* **1992**, *255* (5048), 1113.
(33) Lan, E. H.; Dunn, B.; Valentine, J. S.; Zink, J. I. *J. Sol-Gel Sci. Technol.* **1996**, *7*, 109.
(34) Baca, H. K.; Ashley, C.; Carnes, E.; Lopez, D.; Flemming, J.; Dunphy, D.; Singh, S.; Chen, Z.; Liu, N.; Fan, H.; López, G. P.; Brozik, S. M.; Werner-Washburne, M.; Brinker, C. J. *Science* **2006**, *373* (5785), 337.
(35) Gupta, G.; Atanassov, P.; Lopez, G. P. *Biointerphases* **2006**, *1*, 6.
(36) Rao, G. V.; Lopez, G. P. *Adv. Mater.* **2000**, *12* (22), 1692.

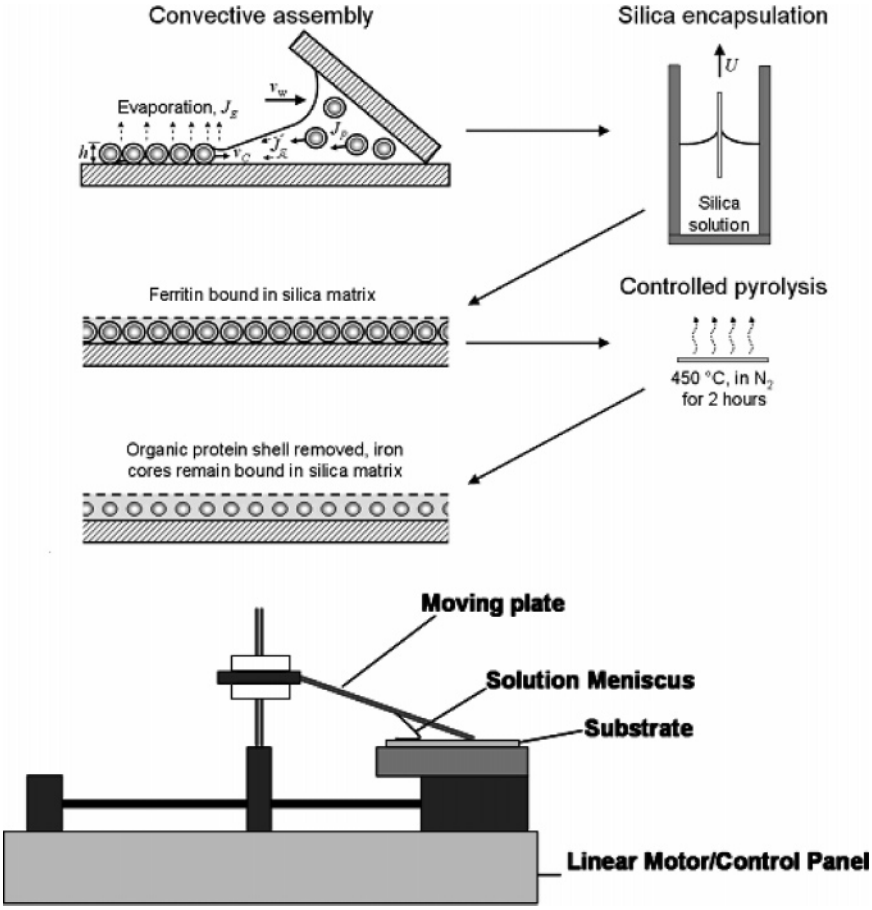

Figure 1. Schematics of the process of assembling ferritin monolayers and converting them into permanent silica films with embedded arrays of iron oxide nanoparticles. The schematic of the experimental setup is shown at the bottom.

of TEM characterization experiment) was studied to analyze the material composition.

Results and Discussion

The major mechanism behind this nanodeposition process is evaporation-induced convective self-assembly of ferritin molecules. Once injected, the bulk of the ferritin solution droplet is held by the capillarity in the wedge between two substrates, while the meniscus stretches out behind. The water evaporates while the solution is spreading, leaving the ferritin molecules gathered at the edge of the meniscus by the convective flux of solvent. Thus, a film of ferritin solution is spread over the substrate plate and forms a solid two-dimensional crystal when finally dried.

The visual appearance of the resulting ferritin films ranged in color from deep orange to translucent, depending on the film thickness. The thickness of the film varies with the ferritin concentration and deposition speed; higher protein concentrations and lower deposition speeds favor the formation of multilayer structures, while too low concentrations and/or high depositions speeds may lead to forming an incomplete monolayer. The results demonstrated that, at properly chosen conditions, ferritin forms quasi-ordered monolayers that are structured in two-dimensional arrays on the substrate. The arrays on the surface consisted of multiple domains of two-dimensional microcrystals. Examples of the typical short-range hexagonal ordering observed in the ferritin monolayers are shown in Figures 2a and 2b. The insert micrograph image at high magnification in Figure 2a clearly shows the hexagonal ordering. The characteristic size of the particles observed in TEM images (by its higher contrast) is 7 nm, which is consistent with the diameter of the ferritin iron core.[27−29] Long-range order was not observed under the conditions studied. Under the deposition conditions used, the ferritin array is obtained as monolayer, as evidenced by the top-view TEM image of the "peel-off" film from the silicon surface (Figure 2b) and Figures 2c and 2e, which are the cross-sectional views under a TEM of an iron oxide nanocluster array obtained after pyrolysis of ferritin coating on silicon, demonstrating monolayer formation of ferritin. The ferritin iron oxide core-to-core distance (array pitch) in the cross-sectional picture is about 10−12 nm, which corresponds to the expected distance for ferritin molecules ordered in a two-dimensional hexagonal pattern.

As mentioned above, varying the ferritin solution concentration and deposition velocity allows controlling the thickness of the short-range ordered ferritin films by means of the number of molecular layers. Figures 3a−3d show a series of SEM microphotographs of tilted samples (tilted at 35°) with single ferritin monolayer coating obtained at different concentrations and deposition velocities. Figure 3a shows a ferritin monolayer obtained with a concentration of 0.5 mg/mL at a coating velocity of 1.6 μm/s. The monolayer in Figure 3c was obtained with a higher concentration of 1 mg/mL along with a relatively faster coating (5.3 μm/s) compared to 1.6 μm/s used in Figure 3a. Similarly, with the increasing concentrations of ferritin solution (increased to 5 and 15 mg/mL), ferritin monolayers were also obtained by increasing the coating velocities accordingly (at 20 and 56 μm/s, respectively) as shown in Figures 3b and 3d. Thus, balancing the concentration and coating velocity can lead to monolayer formation obtained under a range of experimental conditions. Figure 3e shows an SEM micrograph of a sample tilted at 35° with an incomplete monolayer coating of ferritin with 1 mg/mL ferritin solution at 16 μm/s coating velocity, while

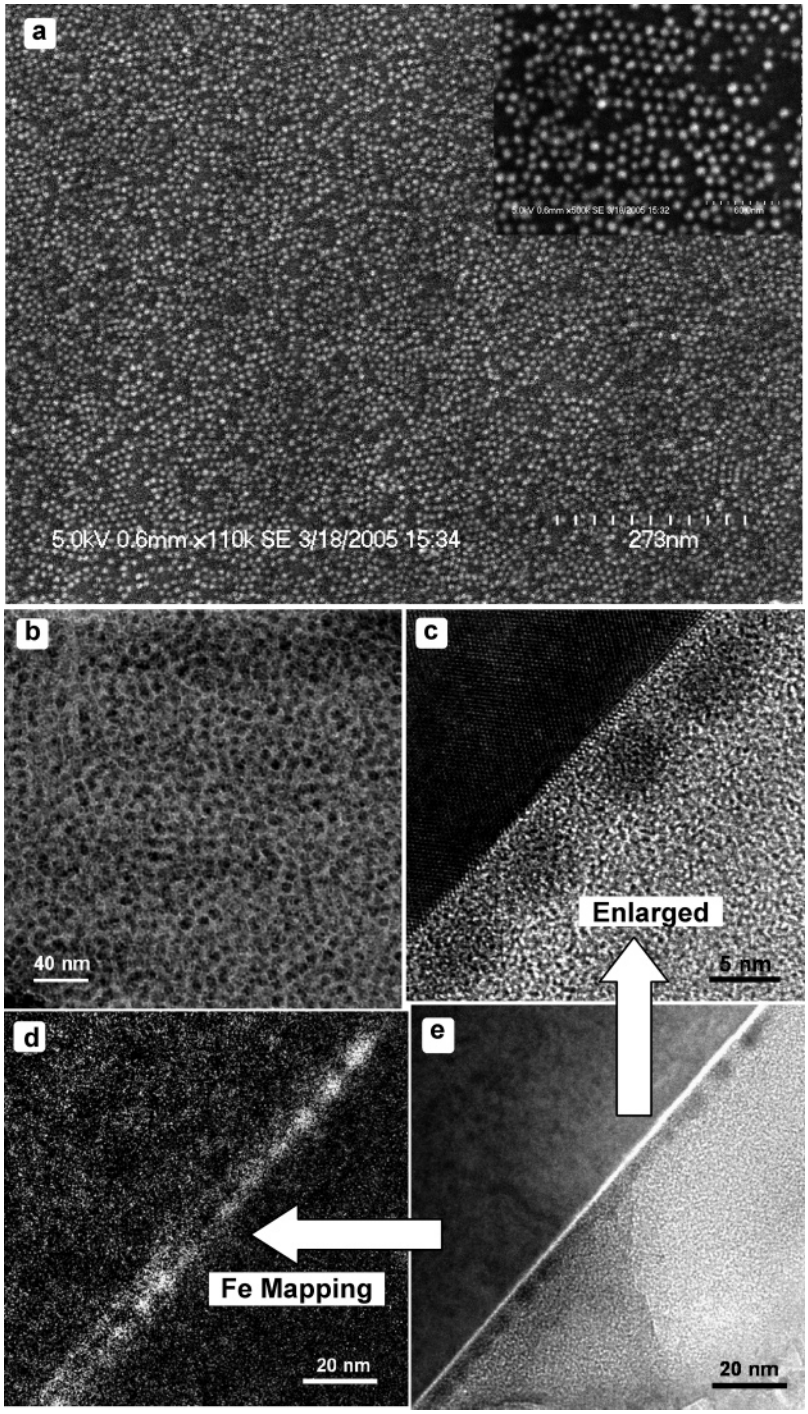

Figure 2. (a) Large-scale SEM microphotograph of ferritin monolayer deposited by convective self-assembly on a silicon wafer. The image in the insert is a high-magnification SEM microphotograph of ferritin monolayer showing hexagonal ordering. (b) TEM image of the ferritin monolayer lifted off the silicon surface to a TEM copper holder. (c), (e) TEM cross-sectional image of an iron oxide nanocluster array obtained after pyrolysis of ferritin monomolecular coating on silicon. (c) is the enlarged part image of (e). (d) TEM cross-sectional image under Fe mapping of iron oxide nanocluster array obtained on silicon.

Figure 3f is a SEM microphotograph with a multilayer coating of ferritin, which was fabricated with the same ferritin solution as Figure 3e (1 mg/ mL) but at a much lower speed of 1.6 μm/s. These two images demonstrate the utility of the spread-coating method in achieving coatings ranging from submonolayer coatings to multilayer coatings.

A model for quantitative interpretation of the colloidal particle layer growth kinetics has been suggested by Dimitrov and Nagayama,[37] and further developed by Prevo and Velev[19] for the interpretation of multilayer formation. According to these authors, for monolayers the velocity of layer growth is equal to the deposition velocity (see Figure 4), v_C, which is given by

$$v_C = \frac{K\phi}{h(1-\epsilon)(1-\phi)} \approx \frac{K\phi}{h(1-\epsilon)} \quad \text{for } \phi \ll 1 \qquad (1)$$

where h is the thickness of the layer ($\sim$ the diameter of a ferritin molecule which is about 12 nm), ϵ is the porosity (volume fraction of the void space) in the layer, and ϕ is the volume fraction of protein in the bulk meniscus in contact with the layer. The protein

(37) Dimitrov, A. S.; Nagayama, K. *Langmuir* **1996**, *12*, 1303.

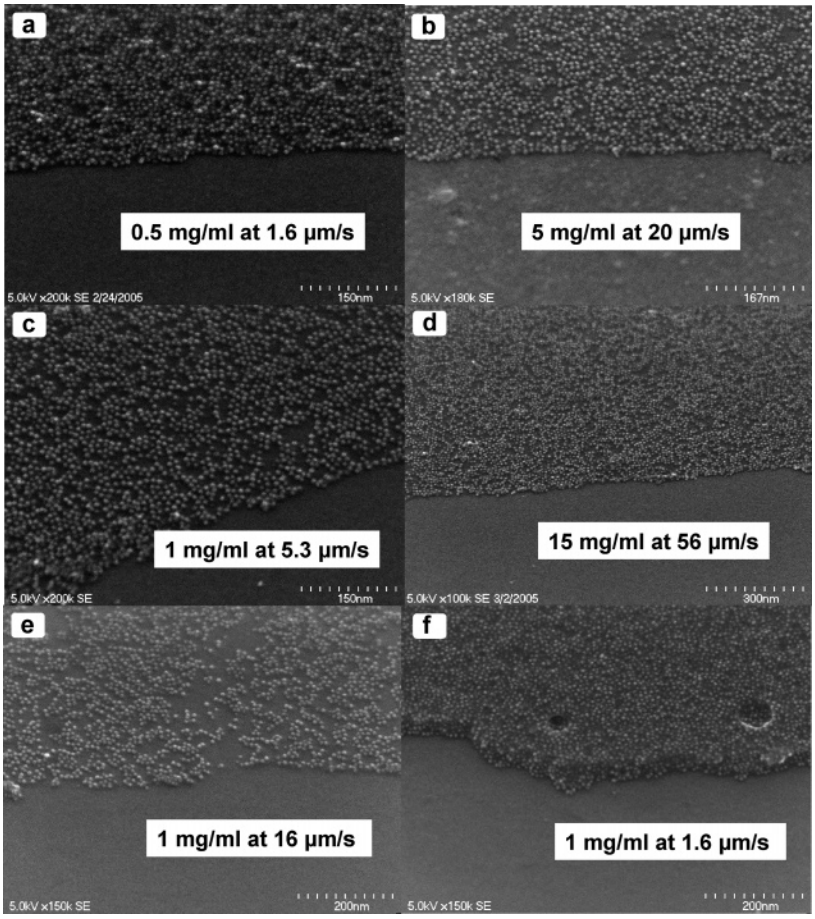

Figure 3. Formation of ferritin monolayers. (a)−(d) 35° tilted SEM micrographs of ferritin monolayer obtained at different concentrations and deposition velocities: (a) with concentration of 0.5 mg/mL at a coating velocity of 1.6 μm/s; (b) with 5 mg/mL concentration at 20 μm/s; (c) with 1 mg/mL at 5.3 μm/s; and (d) with 15 mg/mL at 56 μm/s. (e) is the 35° tilted SEM image of incomplete ferritin monolayer obtained with concentration of 1 mg/mL at 16 μm/s; (f) is the 35° tilted SEM image of ferritin multilayer with 1 mg/mL at coating velocity of 1.6 μm/s.

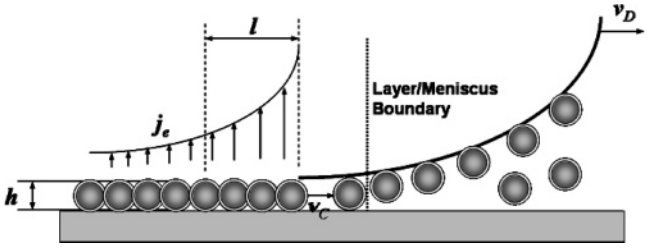

Figure 4. Schematic of the molecule and solvent fluxes in the vicinity of monolayer molecule arrays growing on a substrate. The protein monolayer film is formed at a growth rate v_C; v_D is the deposition velocity of the film (withdraw speed). The j_e is the evaporation flux; l is the drying length of the thin film. For monolayer formation, v_C is equal to v_D.

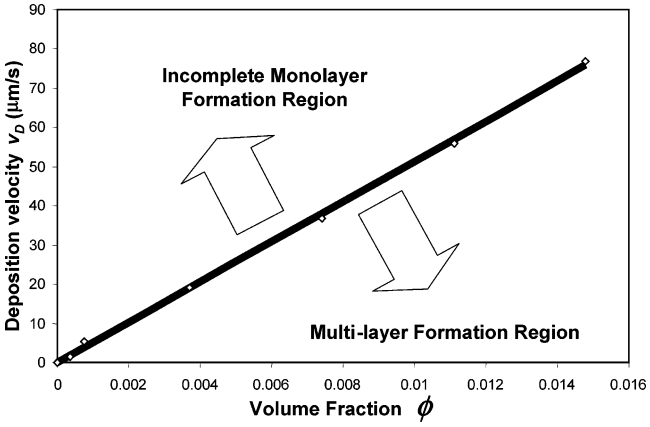

Figure 5. Correlation between deposition velocity and volume fraction for a monolayer ferritin formation. The line indicates the conditions for monolayer ferritin formation. Above the line, the structure formed is an incomplete monolayer. Below the line multilayer deposition is observed.

molecules are transported into the drying region of the monolayer by a convective flux of solvent driven by evaporation. Self-assembly of the protein molecules into ordered two-dimensional structures occurs at the receding meniscus edge before the formation of the hydrated supported film. The coefficient $K = j_e\beta l$ is the product of the evaporation-driven convective velocity j_e, the drying length l, and a dimensionless parameter β that accounts for the interactions between the molecules and the substrate[37] (see also Figure 4). Therefore, the parameter K represents essentially the convective contribution to the molecular transport. Equation 1 suggests that the monolayer growth rate (or deposition velocity) depends linearly on the protein volume fraction in the bulk if the former is low enough (which is our case as the highest protein volume fraction used is 1.48×10^{-2}). Figure 5 presents the correlation between the deposition velocity v_D and the volume fraction ϕ. Plotting v_D vs ϕ (concentration of ferritin has been converted into volume fraction) for ferritin monolayer formation, which has also been traced in Figures 3a−3d, results in a linear relationship. This correlation is obtained at very low volume fractions (<1.5 vol %). It corresponds well to the previously reported correlation for monolayer latex particles

formation[19] in the low volume fraction region. The areas above and below the line in Figure 5 correspond to the incomplete monolayer and multilayer, respectively. The region above the correlation line corresponds to conditions for formation of an incomplete monolayer. The deposition parameters of the coatings shown in Figure 3e correspond to the region above the monolayer line shown in Figure 5. In contrast, the parameters that are used in depositing the film in Figure 3f are from the region below the correlation curve (see Figure 5). The resulting film is a multilayer of ferritin molecules (see Figure 3f). These experimental results also show excellent agreement with the prediction of eq 1. Hence, this relationship allows predicting and controlling the formation of protein monolayers. If the deposition velocity is greater than the value calculated by eq 1, the layer will be an incomplete monolayer; if it is lower, then one obtains multilayers. Only when the deposition velocity is exactly equal to the one predicted by eq 1 is a monolayer formed.

The Peclet number is the ratio of the convective and diffusive terms, which helps to evaluate the impact of these two competitive contributions to the mass transport and the dynamics of the system during convective assembly.[38,39] We define Peclet number that characterizes the monolayer formation by

$$Pe = \frac{K}{D} \tag{2}$$

where $D = 3.2 \times 10^{-7}$ cm^2/s[40] is the ferritin diffusion coefficient in an unbound fluid and infinite dilution corresponding to a molecular radius equal to 6.1 nm. The value for K extracted from the plot in Figure 5 is 3.5×10^{-7} cm^2/s, which gives $Pe = 1.1$. In contrast for large colloidal particles (with radius equal to 550 nm) the number corresponding to a monolayer formation is $Pe = 275$. The direct comparison between protein solutions and latex suspensions using Pe numbers alone however might not be fully representative. The numbers cited above are for isolated particles in an infinite fluid. In the deposition experiment, the protein molecules and/or latex particles are in a confined space and the interactions with the substrate become increasingly important and very different for the two species. Also the concentration at the layer/meniscus boundary (see Figure 4) sharply increases, which leads to intermolecular and interparticle interactions. Both effects will change the diffusion coefficients of the protein and the latex particles. This change could be substantial and very different for the two species. These interactions will have a strong impact on the effective values of the diffusion coefficients[41,42] but they are not accounted for in the above estimates of Pe where we have used bulk values. The detailed investigation of the diffusivity of interacting molecule in confined spaces is not trivial and is outside the scope of the present study. The monolayer formed by proteins is less ordered and occurs at lower volume fractions than in the case of larger colloidal particles,[19] which suggests stronger attractions and protein−substrate interaction. Therefore, while eq 1 is valid both for large colloids and small protein molecules, the governing parameter K may differ substantially (through β) for both cases.

The sample composition and structure were also confirmed by energy-dispersive spectroscopy (EDS) mapping (obtained as a part of TEM characterization experiment). EDS mapping (Figure 6, "Fe") proved that the sample composition consists mainly of oxidized iron. Three peaks appeared at 0.7, 6.4, and 7.1 keV and were identified as Fe(II) and Fe(III). The oxygen peak corresponds to the oxygen from the iron oxides and the oxygen component in the organic components (protein chains). The carbon peak in the mapping is largely from the protein organic part of the ferritin shell. Some other peaks observed in EDS are primarily associated with the instrument, such as the copper peak from the copper TEM sample substrate, and the silicon peak from the silicon detector. The pattern of the iron-containing layer in Fe mapping (Figure 2d) is consistent with a ferritin monolayer, which is shown in the native cross-sectional view: ferritin array only on the substrate (Figures 2c and 2e). The interfaces in Si mapping (not shown) and Fe mapping (Figure 2d) are at the same positions, which indicates that a planar film containing iron nanoparticles lies in close proximity to the silicon substrate. Furthermore, the distance separating the iron clusters signal in Fe mapping is consistent with the intermolecular distance in ordered ferritin monolayer.

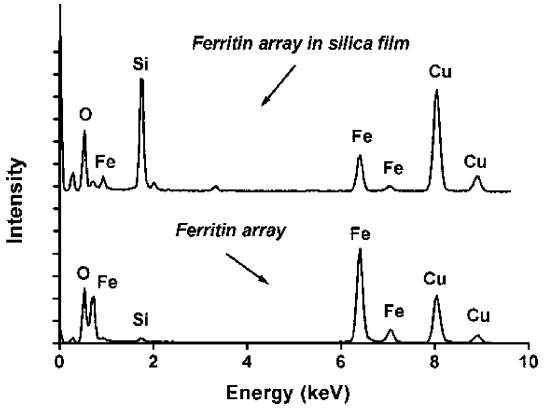

Figure 6. EDS of ferritin sample from Figure 2 (ferritin array before pyrolysis) and Figure 7 (ferritin array coated with silica film before pyrolysis).

The ferritin films deposited on the solid substrate were encapsulated in a silica matrix grown in situ by sol−gel technique. We hypothesize that the absorbed protein molecules do not rearrange on the surface during the dip-coating process due to a variety of factors, possibly including strong van der Waals attraction and the coagulating action of the silica solution, which contains high concentration of ionic species. Figure 7a depicts the layer of ferritin after incorporation into the silica matrix. The ordered structure of the monomolecular layer was preserved after encapsulation.

The organic protein shell of the ferritin was then removed by controlled pyrolysis. The remaining iron cores encapsulated in silica retained their original ordering achieved via the convective assembly. An array of iron oxide nanoclusters derived from the ferritin monolayer encapsulated in silica after pyrolysis is shown in Figure 7b. Under the suggested conditions of controlled pyrolysis,[10] the protein shell is completely decomposed, but the order and spacing of the original ferritin layer were successfully preserved in the resulting array from iron cores as evidenced by the high-magnification cross-sectional image (Figure 7c). The particles appear to have less pronounced boundary contrast as compared to those from the ferritin cross-sectional picture shown in Figures 2c and 2e. This effect is probably due to the increased resistance of the sample caused by the silica coating on the ferritin molecules, which hinders the electron beam transmission by effectively increasing the film thickness.

The EDS spectra taken before and after silica encapsulation (with TEM) clearly show that the iron and oxygen peaks did not change significantly, while a 30-fold increase in the silicon peak

(38) Batchelor, G. K. *J. Fluid Mech.* **1976**, *74*, 1.
(39) Felderhof, B. U. *J. Phys. A.* **1978**, *11* (5), 929.
(40) Lin, H.; Petsev, D. N.; Yan, S. T.; Thomas, B. R.; Vekilov, P. G. *Cryst. Growth Des.* **2001**, *1* (1), 73.
(41) Petsev, D. N.; Denkov, N. D. *J. Colloid Interface Sci.* **1992**, *149* (2), 329.
(42) Huerta, A.; Naumis, G. G.; Wasan, D. T.; Handerson, D.; Trokhymchuk, A. *J. Chem. Phys.* **2004**, *120* (3), 1506.

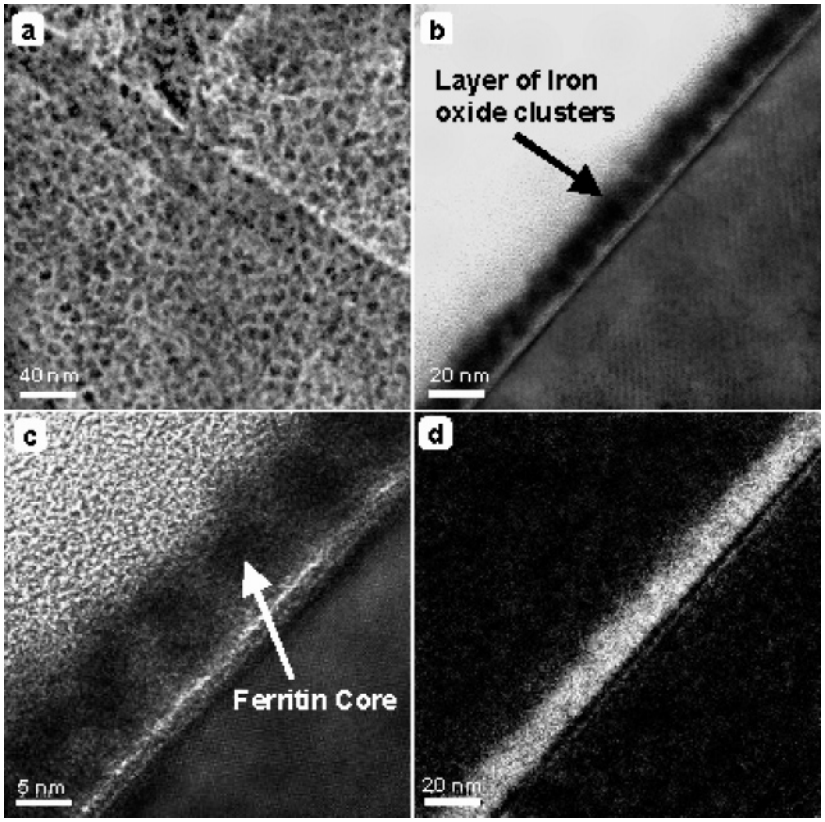

Figure 7. (a) TEM image of silica film incorporating the ferritin monolayer and consequently transferred to TEM copper grid. (b) TEM cross-sectional image of iron oxide nanocluster coated with silica film after pyrolysis. (c) Enlarged section of (b). (d) TEM cross-sectional image under Fe mapping.

reflects the presence of the silicate gel that was deposited on the ferritin array (Figure 6). EDS spectra obtained in both TEM and SEM experiments were practically identical, showing significant presence of Si in the coating. These EDS spectra provided a direct confirmation of the silica coating over the ferritin layer. All results confirm the formation of a silica film with embedded iron oxide nanocluster arrays derived from ferritin.

Conclusion

This paper demonstrates the formation of short-range ordered iron oxide nanoparticle arrays by rapid and controlled deposition of 2D ferritin arrays on silicon or glass substrates and their transformation into solid bio-inorganic nanocoating via silica encapsulation. By optimizing the conditions, we can control the formation of monolayer ferritin arrays using this simple convective self-assembly process. The iron nanocores derived from ferritin arrays have been well-preserved as a uniform layer of intact particles rather than segregated entities after the protein shell removal. The principal method for controlled deposition of protein layers is evaporation-induced convective assembly. This approach efficiently combines the convective assembly for deposition of structured ferritin monolayers and traditional dip-coating method for the inexpensive silica precursor. It has promise of developing into a high-throughput nanocoating technology. This paper also establishes a linear correlation between two deposition parameters: concentration or volume fraction and deposition velocity that allow preparation of ferritin monolayers in a well-defined fashion. A particular advantage of this method is the potential to make a large homogeneous monolayer of ferritin and other large proteins on the solid substrates. In addition to that, when nanoscale patterning of the substrate upon which the protein arrays are formed is employed, it is a possible method to direct the self-assembly process toward the spacing and orientation of the arrays. The ferritin cores could be modified to have single magnetic domain properties and the solid nanocoating encapsulating these magnetic nanoparticles could be a precursor for high-density magnetic storage.[43] Ultimately, this technique could give an opportunity to design robust 2D nanocluster arrays of desired architecture for a variety of applications ranging from magnetic memories to quantum dots to catalytic surfaces.

Acknowledgment. The authors are grateful for the financial support from the Office of Naval Research N000140210169 and NCSU NSF Science and Technology Center for CO_2-based Solvents and Processes under Agreement CHE-9876674. We thank Dr. Richard Watt for ferritin purification and Dr. G. V. Rama Rao for silica gel preparation and helpful discussions. We also thank Dr. Huifang Xu and Yingbing Jiang for their help with TEM imaging.

LA062891F

(43) Yuan, Z.; Atanassov, P.; Alsmadi, A. M.; te Velthuis, S. G. E.; Welp, U.; Hammetter, C. I.; Hjelm, R.; Nakotte, H. *J. Appl. Phys.* **2006**, *99* (1), 08Q509.